



Journal of Applied Sciences

ISSN 1812-5654

science
alert

ANSI*net*
an open access publisher
<http://ansinet.com>

Burst Pressure Estimation of Corroded Pipeline with Interacting Defects Using Finite Element Analysis

S. Karuppanan, A.S. Aminudin and A.A. Wahab
Department of Mechanical Engineering, Universiti Teknologi PETRONAS,
Bandar Seri Iskandar, 31750 Tronoh, Perak, Malaysia

Abstract: Failure due to corrosion defects has been the major problem in maintaining pipeline integrity. The loss of metal due to corrosion usually results in localized pits with various depth and irregular shapes which occur on its external and internal surfaces. An interacting defect is one that is located sufficiently close and able to interact with neighbouring defects in an axial or circumferential direction. The maximum allowable pressure that can be sustained in a pipeline with interacting defects is lower than it is in single defect due to interaction of neighbouring defects. Several methods are available to assess the corrosion metal loss defects in order to evaluate the Fitness-for-Services (FFS) of the corroded pipeline. In this study, extensive finite element simulations have been carried out to determine the burst strength of corroded pipeline with interacting defects. The Finite Element Analysis (FEA) showed that the failure pressure results of corroded pipeline with interacting defects were higher than the empirical values obtained from DNV-RP-F101 Code.

Key words: Pipeline assessment, burst pressure, interacting defects

INTRODUCTION

Pipeline systems are generally a convenient means for transferring oil and gas onshore or offshore due to the economic and safety reasons. However, with increasing age, the pipeline integrity can be affected by a range of corrosion mechanisms. Corrosion is defined as the destruction or deterioration of a material because of its reaction with the environment (Fontana and Greene, 1987). Pipeline is exposed to both internal and external corrosion. The internal corrosion of pipeline is due to the harsh condition of hydrocarbon fluid which includes the presence of CO₂, H₂S and organic acid (Kusha *et al.*, 2011). External corrosion occurs due to the extreme conditions of the surrounding environment when the preventive measures failed; such as older/degraded coating or poorly coated pipeline (Shafiq *et al.*, 2010; Chouchaoui and Pick, 1996). This will result in metal loss at the corroded location in the pipeline and may eventually lead to its failure. The impact of corroded pipeline problems cause economic consequences; such as reduced operating pressure, loss of production due to downtime, repairs or replacement and consequently increase of costs.

Thus, several pipelines systems are kept in operation even though they have shown signs of corrosion based on the data obtain from the corrosion management,

inspection and monitoring systems, i.e., intelligent pig. The continued operations of these pipelines are basically done after the FFS assessment to determine their residual strength and recalculation of the maximum allowable internal pressure of the product being transferred (Netto *et al.*, 2005). The structural integrity assessment of corroded pipeline has become vital to assist engineers to make wise decision toward replacing or repairing a pipeline. It is essential to ensure the continued safe operation and non hazardous incidences which might affect the life and the environment. Various methods for assessing pipeline corrosion are available and commercially have been practiced by the industry, such as ANSI/ASME (1991) For a more realistic way of pipeline corrosion representation (Silva *et al.*, 2007), new criteria were developed, such as RSTRENG Effective Area (Kiefner and Vieth, 1989) and DNV RP-F101 (Netto *et al.*, 2005). These methods include the specification dealing with the effects of the interacting defects. Even though these codes have been used widely for assessing the integrity of in-service pipelines, they are known to be conservative (Belachew *et al.*, 2009). In other words, pipelines which have been assessed by these codes for the purpose of FFS analysis probably would lead to either unnecessary maintenance or premature replacement.

The occurrence of corrosion is divided into several categories, namely individual pits, colonies of pits, general wall-thickness reduction, or a combination of

these (Lee *et al.*, 2005). An interacting defect is defined as the one that interacts with neighbouring defects in an axial or circumferential direction (DNV, 2004). For colonies of corrosion defects, as the distance between the defects decreases, the defects will begin to interact, resulting in reduced burst strength of the pipeline. A more reliable defect assessment method is needed due to the conservatism involved in the available assessment method (Belachew *et al.*, 2011). This is an approach to understand the effect of interacting defects toward the pipeline burst strength in a more reliable and convenient method other than performing experimental testing.

Therefore, the modelling of the problem using FEA method can assist engineers to assess the burst strength of pipeline with interacting defects. The objective of this study is to estimate the burst pressure of corroded pipeline due to interacting corrosion defects by the means of FEA. The analysis is performed by nonlinear FEA simulation using ANSYS Software. The effect of different spacing between two defects aligned in longitudinal direction to their failure pressure will be studied. Then the FEA results will be compared to the numerical values calculated from the DNV RP-F101 code.

DNV-RP-F101 CODE

DNV-RP-F101 method for interacting defects (part A) was used in this study to estimate the burst pressure of the corroded pipeline. In DNV procedure, all the defects that are supposed to interact are projected onto a longitudinal line. The metal loss is represented by the maximum defects depth and the projected defects length.

In the case of overlapped defects, they are combined to form composite defects. The formation of combined defects is estimated by taking the combined length and the depth of the deepest defect. For combination of overlapping internal and external defects, the depth of the composite defect is the sum of maximum depth of those two defects. Each defect or composite defects (i) with

length (l_i) and depth (d_i) is treated as a single defect and failure pressure (p_i) is defined based on the expression below:

$$p_i = \gamma_m \frac{2f_u(1 - \gamma_d(d_i/t)^*)}{(D-t) \left(1 - \frac{\gamma_d(d_i/t)^*}{Q_i}\right)} \quad i=1, \dots, N \quad (1)$$

where, N is the is number of projected defects, D is the nominal outside diameter (mm), t is uncorroded measured pipe wall thickness, f_u is the ultimate tensile strength, γ_m is the partial safety factor for model prediction, γ_d is the partial safety factor for corrosion depth and Q_i is the length correction factor for individual defect, given by:

$$Q_i = \sqrt{1 + 0.31 \left(\frac{l_i}{\sqrt{D}t}\right)^2} \quad (2)$$

The correction depth over thickness ratio is determined by the following expression:

$$(d_i/t)^* = (d_i/t)_{meas} + \epsilon d StD[d_i/t] \quad (3)$$

where, ϵd is the factor for defining a fractal value for the corrosion depth and $StD[d_i/t]$ is the standard deviation of the measured (d_i/t) ratio.

Next, the combinations of adjacent defects were investigated. Take note that for combined defects, the effective length (l_{nm}) is the total length of the projected defects and the spacing between the defects (Fig. 1). For defects from n to m, the effective length is given by:

$$l_{nm} = l_m + \sum_{i=n}^{i=m-1} (l_i + s_i) \quad n, m = 1 \text{ and } N \quad (4)$$

where, l_i is the longitudinal length of an individual defect, s_i is the projected distance between the two adjacent defects. Meanwhile, the effective depth (d_{nm}) of combined defects formed from all of interacting defects from n to m (Fig. 1) is calculated as below:

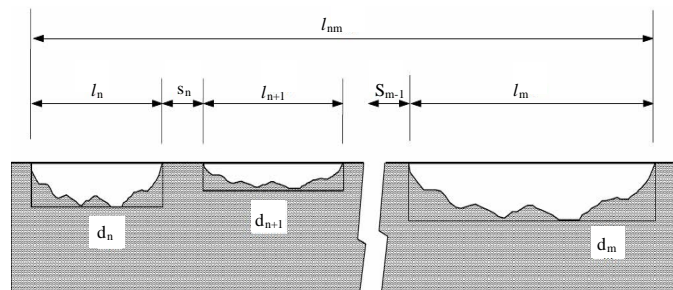


Fig. 1: Combined length of all combination of adjacent defects (DNV, 2004)

$$d_{nm} = \frac{\sum_{i=n}^{i=m} d_i l_i}{l_{nm}} \quad (5)$$

where, d_i is the depth of an individual defect.

The failure pressure (p_{nm}) of the combined defects from n to m is calculated by replacing (l_i) and (d_i) with (l_{nm}) and (d_{nm}) in Eq. 1 and 2. The minimum value, calculated for all single and combined defects, is taken as the failure pressure for the current projection line.

According to the DNV interaction rules, there is no interaction if the longitudinal (s_l) and circumferential (s_c) distances between the defects satisfy the following conditions:

$$\text{Longitudinal limit } (s_l) = 2.0\sqrt{Dt} \quad (6)$$

$$\text{Circumferential limit } (s_c) = \pi\sqrt{Dt} \quad (7)$$

FINITE ELEMENT METHOD

The models were developed from API 5L X65 steel alloy with the nominal dimension of 300 mm diameter, 20 mm wall thickness and 1000 mm section length. Meanwhile, the defects geometry was selected to cover the following basic parameters: normalized defect depth (d/t of 0.1, 0.2, 0.3, 0.4, 0.5, 0.6, 0.7 and 0.8), normalized defects spacing of 0.5, 1.0, 2.0, 4.0 and 8.0). A total of 40 models with internal defect geometry characterized by a length of $l = 100$ mm and width of $c = 90$ mm were generated.

Since the problem involved two equally shaped defects, only a quarter of a full pipe was generated based on the symmetric condition. This was to reduce the size of the model and hence to reduce the processing time of the simulation. These models were meshed with SOLID95 elements which are defined by 20 nodes having three degrees of freedom at each node, which are translations in the nodal x , y and z directions. SOLID95 brick elements were chosen because they can tolerate irregular shapes without as much loss of accuracy and have compatible displacement shapes and are well suited to model curved boundaries. These elements also have plasticity, stress stiffening, large deflection and large strain capabilities. Two layers of elements were used at the defect region through its ligament. Fine meshes were utilized at the defect region while coarser meshes were utilized farther from the corrosion defect region, as shown in Fig. 2.

One end of the pipe was fixed by constraining all degrees of freedom as to simulate the enclosed end of the pipe. The symmetric boundary condition was imposed to the other end of the pipe (which is closer to the defect)

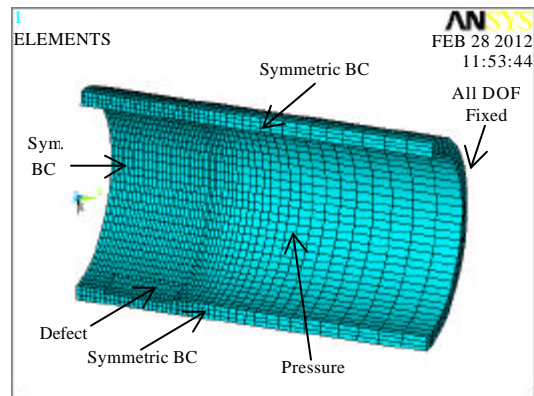


Fig. 2: Finite element model of the defect, mesh and boundary conditions

and also to the sides of the pipe. The inner wall of the model is then subjected to incremental internal pressure loading during the simulation. Figure 2 shows the boundary conditions imposed on the model in this study.

In this study, nonlinear analyses were carried out. In order to correctly evaluate the corroded pipe, appropriate failure criterion should be established to decide the failure point during the simulation (ANSI/ASME, 1991). The failure/stopping criterion of this simulation was when the Von-Mises stress distribution across the entire ligament of the pipe reaches the ultimate tensile stress, 530.9 MPa. The pipe is considered to fail when this condition is achieved. As the pressure applied on the internal surface of the pipe increased, the critical stress starts to propagate along the edge of the defect and spread around the defect area. The assessment of the critical stress through the entire ligament was carried out by considering several points at the critical defect area.

RESULTS AND DISCUSSION

Figure 3 shows the results for an example case of $d/t = 0.2$ and $s/\sqrt{Dt} = 0.05$. The critical section was observed along the edge of the defect. The critical stress starts from this edge and spreads around the defect area. The simulation is terminated when the Von Mises stress value through the thickness of this critical section reaches ultimate tensile stress value of 530.9 MPa.

The failure pressure obtained in this study was normalized with the failure pressure of an intact pipe obtained using the FEA method. The failure pressure of an intact pipe found by FEA method was 90 MPa. Figure 4 shows the results of normalized corroded pressure versus normalized defect spacing, obtained by FEA and DNV code, for an example case of $d/t = 0.4$.

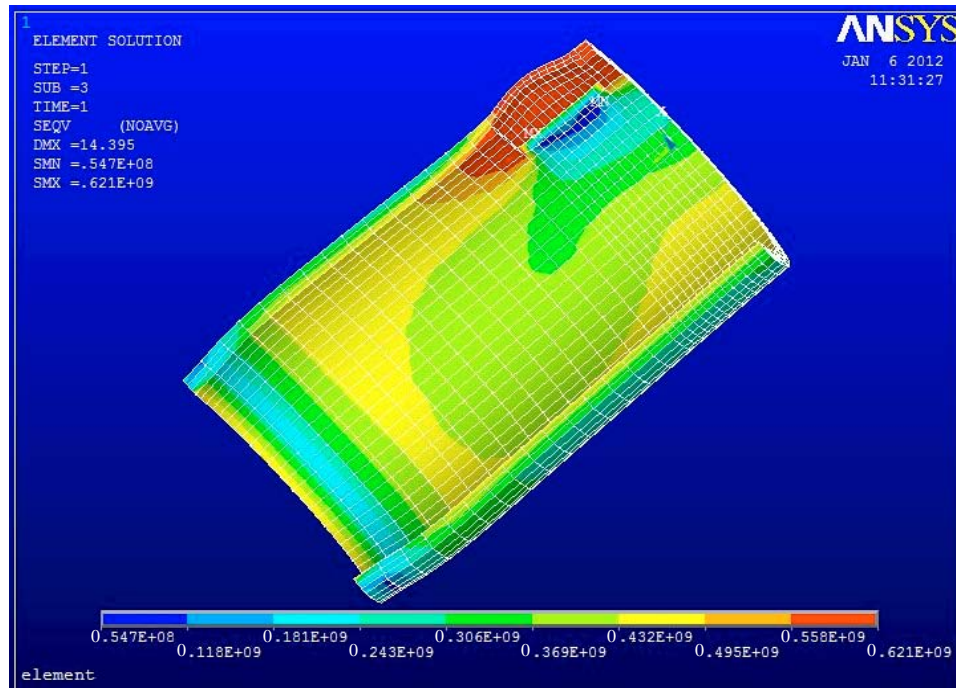


Fig. 3: Von Misses stress distribution for $d/t = 0.2$ and $= 0.5$ (internal view)

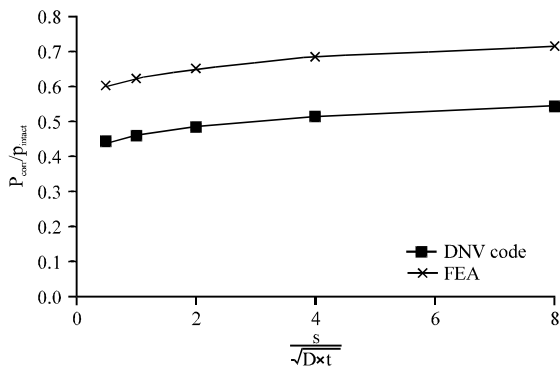


Fig. 4: Effect of defect spacing on burst strength for $d/t = 0.4$

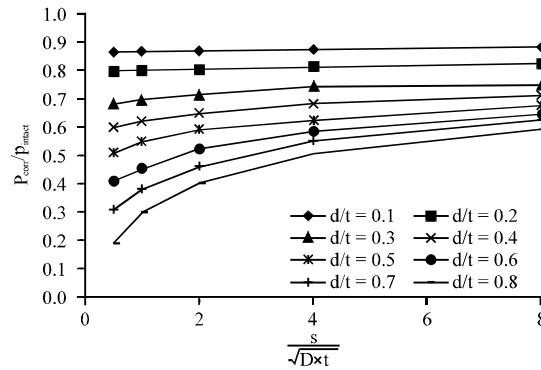


Fig. 5: Effect of defect depth and defect spacing on the failure pressure using FEA

Generally, the results obtained from FEA are higher compared to the values obtained using the DNV Code. The non linear finite element analyses yielded results which have similar trend with the empirical solution using the DNV Code. These observations apply for other cases as well.

Figure 5 shows the effect of defect depth and defect spacing on the failure pressure of pipes with defects using FEA. Generally, as the distance between the defects decrease, the maximum allowable corroded pressure will also decrease. Furthermore, as the depth of the defects increase, the failure pressure will decrease.

The effect of spacing between the defects is not significant for the shallow defects as was observed for $d/t = 0.1$ and $d/t = 0.2$. In other word, the effect of interaction on the pipe failure pressure for defects with depth of less than 20% of pipe wall thickness is minimal. As the defect depth increase, the effect of interaction becomes obvious. For d/t ratios of 0.3 to 0.8, the gradual drop in failure pressure was observed when the normalized spacing is less than 4. This shows that, when the spacing between the defects is small, they start to interact with each other and reduce the maximum allowable corroded pipe pressure. The drastic drop in

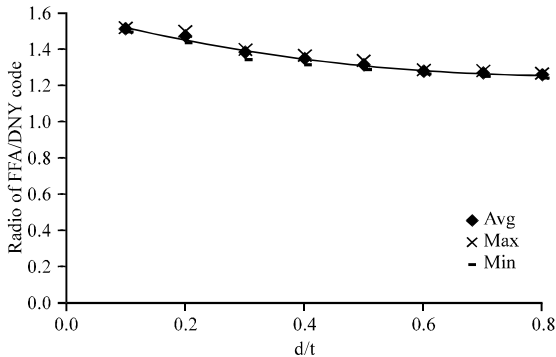


Fig. 6: Effect of defect depth on the ratio of FEA results over DNV Code results

failure pressure was observed for $d/t = 0.8$. The effect of interaction is more critical for deeper defects.

The results from FEA is consistently higher than the DNV Code results. This was due to the safety factor applied in the empirical calculation which yields a lower corroded pipe failure pressure as to avoid reaching the exact failure pressure during standard operating condition. Figure 6 shows the effect of the defect depth on the ratio of FEA results over the DNV Code results. This factor is not a fixed value since the multiplication factor in FEA was not the same for every cases of defects depth. This was due to stress concentration at the edges of the defects during the simulation process. The deeper the defect depth, the higher the stress concentration at the edge of the defect. Since the remaining pipe wall thickness is small, the stress distribution on the entire ligament of the edge easily reaches the failure criterion. Figure 6 shows a decreasing trend of the factor as the depth of the defects is increasing. The best plot on the graph is based on the average value of the ratio of the FEA results over the DNV Code results. The ratio can be expressed as a function of:

$$\text{Ratio} = 0.481(d/t)^2 = 0.805(d/t)+1.583$$

CONCLUSION

Consideration for maintenance or replacement of corroded pipeline is crucial because it affects directly to the cost of the firm. The existing codes that have been widely practiced by the industry are too conservative. This may lead to unnecessary maintenance or premature replacement of corroded pipeline. Therefore, the FEA is one of the reliable methods to assess the burst strength of the corroded pipeline. Burst strength of pipeline with interacting corrosion defects can be accurately predicted by FEA using ANSYS software. The application of FEA can reduce the conservatism involved in the conventional

methods. From this study, the ratio of FEA results over the DNV Code results is a multiplication factor expressed by a function below:

$$\text{Ratio} = 0.481(d/t)^2-0.805(d/t)+1.583$$

REFERENCES

ANSI/ASME, 1991. Manual for Determining the Remaining Strength of Corroded Pipelines: A supplement to ASME B31 Code for Pressure Piping. American Society of Mechanical Engineers, USA., pp: 55.

Belachew, C.T., M.C. Ismail and K. Saravanan, 2009. Capacity assessment of corroded pipelines using available codes. NACE Asia Pacific, Kuala Lumpur. http://eprints.utp.edu.my/1772/1/NACE_Conference_Paper.pdf

Belachew, C.T., M.C. Ismail and S. Karuppanan, 2011. Burst strength analysis of corroded pipelines by finite element method. *J. Applied Sci.*, 11: 1845-1850.

Chouchaoui, B.A. and R.J. Pick, 1996. Behaviour of longitudinally aligned corrosion pits. *Int. J. Pressure Vessels Piping*, 67: 17-35.

DNV, 2004. Recommended practice RP-F101 for corroded pipelines. Det Norske Veritas, Norway.

Fontana, M.G. and N.D. Greene, 1987. *Corrosion Engineering*. 3rd Edn., McGraw-Hill, New York.

Kiefner, J.F. and P.H. Vieth, 1989. A Modified Criterion for Evaluating the Remaining Strength of Corroded Pipe. Pipeline Research Committee, American Gas Association, USA.

Kusha, A., M.R. Mogadam and F.S.M. Meysam Abutorabi, 2011. Material selection in oil production unit in one of Iranian onshore project. *J. Applied Sci.*, 11: 2000-2005.

Lee, Y.K., Y.P. Lim, M.W. Moon, W.H. Bang, K.H. Oh and W.S. Kim, 2005. The prediction of failure pressure of gas pipeline with multi corroded region. *Mater. Sci. Forum*, 479: 3323-3326.

Netto, T.A., U.S. Ferraz and S.F. Estefen, 2005. The effect of corrosion defects on the burst pressure of pipelines. *J. Constr. Steel Res.*, 61: 1185-1204.

Shafiq, N., M.C. Ismail, C.T. Belachew, S. Karuppanan and M.F. Nuruddin, 2010. Burst test, finite element analysis and structural integrity of pipeline system. Hydrocarbon Asia's Engineering and Operations Convention, Kuala Lumpur, Malaysia. <http://www.pm-pipeliner.safan.com/mag/ppl0910/t38.pdf>

Silva, R.C.C., J.N.C. Guerriero and A.F.D. Loula, 2007. A study of pipe interacting corrosion defects using FEM and neural networks. *Adv. Eng. Softw.*, 38: 868-875.